Pollack Periodica • An International Journal for Engineering and Information Sciences

21 (2026) 2, 29–36

DOI: 10.1556/606.2025.01379

ORIGINAL RESEARCH PAPER

Numerical investigation of a dual- purpose solar collector using different liquids

Mustafa Moayad Hasan[1,2*] and Krisztián Hriczó[1]

[1] Department of Analysis, Institute of Mathematics, Faculty of Mechanical Engineering and Informatics, University of Miskolc, Miskolc, Hungary

[2] Department of Mechanical Power Techniques, Basra Technological Technical Institute, Southern Technical University, Basra, Iraq

Received: March 25, 2025 • Revised manuscript received: May 8, 2025 • Accepted: May 8, 2025
Published online: September 25, 2025

ABSTRACT

This study examines the impact of various heat transfer fluids - water, Therminol VP-1, and Dowtherm A - on the efficacy of a dual-purpose solar collector. Using ANSYS Fluent for computational fluid dynamics, analysis was conducted under constant parameters, including inlet temperatures and solar energy. Results showed that the outlet air temperature increased by 6.67% for Therminol VP-1 and 6% for Dowtherm A, while exit liquid temperatures rose by 14.33% and 13.7%, respectively. Total heat gain and thermal efficiency improved by 21.5% and 20%, respectively, when using Therminol VP-1 and Dowtherm A compared to water. This study is novel in being the first to evaluate these two oil-based fluids alongside water in a dual-purpose solar collector. Overall, Therminol VP-1 and Dowtherm A enhance the thermal efficiency of the dual-purpose solar collector, making them effective alternatives to water as heat transfer fluids.

KEYWORDS

dual-purpose solar collector, different heat transfer fluid, Therminol VP-1, Dowtherm A, computational fluid dynamics simulation, thermal performance

1. INTRODUCTION

The necessity for renewable energy is highlighted by numerous factors, including the dwindling supply of fossil resources, rising energy prices, and ecological challenges [1, 2]. Solar is a clean energy source distinguished by its availability, efficient delivery for power production, and versatility across diverse applications [3, 4]. In the solar heating sector, Flat Plate Solar Collectors (FPSCs) represent the primary devices for harvesting the solar radiant heat [5]. These devices' manufacturing, maintenance, and operating expenses are very low, making them the most desirable choice among other collectors [6]. The small amount of the heat transmission coefficient that exists between the absorbent plate and the circulating fluid contributes to reduced thermal efficiency in FPSCs, constituting a major downside [7]. Improving this criterion has been of concern to academics for decades. Various enhancement strategies involving modifications to design aspects, examination of different heat transfer fluids, and integration of thermal storage systems are being undertaken by multiple researchers to boost the heat functionality of FPSCs [8]. However, combining air and water solar heaters into a singular, innovative device is a viable development, as it can augment the yearly use of solar energy, achieve elevated temperatures with substantial heat production, and decrease both space requirements and prices by 50% [9]. This bi-fluid solar heater is a hybrid kind of FPSCs called a Dual-Purpose Solar Collector (DPSC). It can deliver hot air and water concurrently or independently as it comprises air and water sections. The DPSC was constructed and analyzed for the first time by Tabrizi et al. [10]. They found that DPSC performs better than the stand-alone collector with an increment of 10% in efficacy and

*Corresponding author.
E-mail: hasan.mustafa.moayad@student.uni-miskolc.hu, mustafa.hasan@stu.edu.iq

output temperature of the air section compared to a single air heater. The various design configurations and operating aspects of the DPSC, highlighting their significant findings, have been previously reviewed in our earlier study [6].

The efficiency of solar heaters is highly dependent on the Heat Transfer Fluid (HTF) flowing inside the collector's tubes as it captures the radiant thermal energy from sunlight while moving through the glass. It plays a vital role in multiple applications, including the heating and cooling buildings, automobiles, and biomedicine [11]. While water is the predominant HTF utilized in FPSCs, it presents limitations due to its inferior thermal properties and challenges related to freezing and scale formation [12, 13]. Recent studies have explored the integration of nanofluid suspensions of tiny particles with excellent thermal conductivity into liquid HTFs to boost the thermal transport capabilities of the base fluid [14, 15]. On the other hand, hybrid nanofluids, which consist of various types of nanoparticles, have emerged as advanced alternatives to mono nanofluids, offering improved thermophysical properties [16]. Ethylene-Glycol (EG) or Propylene Glycol (PG) can be blended with water in varying ratios to create a new HTF. These mixtures are applicable in cold and hot climates because glycol can increase the boiling temperature of water and lower the freezing temperature of water. The main disadvantage of glycol liquids is that the thermal conductivity is less than that of water by a factor of three [17]. In addition to water and glycol mixtures, other fluids are utilized, including molten salt (HITEC), mineral oil, Therminol, and Dowtherm oil, which are utilized as HTF in solar thermal applications owing to their beneficial thermo-physical characteristics. Arslan and Günerhan [18] theoretically examined three liquids (Dowtherm A oil, air, and molten salt) in a Parabolic Trough Collector (PTC) energetically and exegetically. The study indicated that molten salt possesses the highest energy performance within its temperature range of 250 °C–550 °C. Moreover, molten salt exhibited the highest exergy efficiency at higher temperatures, reaching a maximum of 41.19% at 422 °C. Balamurali and Natarajan [19] investigated the thermal performance of FPSC for domestic water heating in Mumbai, India, utilizing three HTFs (Dowtherm A, Molten salt, and Therminol VP-1) along with varying internal groove profiles (plain, rectangular, and trapezoidal). Therminol VP-1 revealed superior performance attributed to its thermo-physical properties, particularly when integrated with a trapezoidal groove profile. An optimal performance metric, including a maximum output temperature of 51.6 °C, a thermal gain of 1478 W, and an efficacy of 77.3% was achieved, exceeding the conventional and rectangular patterns by 1.01% and 1.003%, respectively. Narayana and Kalla [20] numerically investigated the thermal performance of FPSC comprising 15 tubes employing ANSYS Fluent software. Three different HTFs (Dowtherm, water, and mineral oil) have been examined in their study to select the best fluid for the FPSC. The effects of various liquid flow rates and tube lengths on the exit temperature were tested and compared. Mineral oil and Dowtherm outperformed water due to their smaller heat capacity. Mineral oil achieved a highest temperature of 448.305 °C at a mass flow rate of 5×10^{-5} kg s^{-1}. They concluded that mineral oil is appropriate for the industrial usage of FPSCs. On the other hand, nanoparticles can enhance not only water but also synthetic oils, thereby increasing their thermal behavior. Alsarraf et al. [21] numerically simulated a spiraled absorbent tube in FPSC using a hybrid MgO-Multi-Walled Carbon NanoTube (MWCNT)/Therminol VP-1 nanofluid. ANSYS software was implemented under turbulent conditions and for various operating scenarios. The findings demonstrate that energy and exergy efficiencies improve by increasing the Reynolds number and nanoparticle volumetric percentage. Additionally, Kalaiarasi et al. [22] designed a solar air collector featuring tubes made of copper containing Therminol-55, premium synthetic oil. These tubes act as sensible heat storage units to enhance the outlet air temperature. Experiments comparing the conventional and novel air heaters indicated that the innovative design achieved a peak energy efficacy of 67.7% at a flow rate of 0.028 kg s^{-1}, outperforming the conventional heater by providing superior and more consistent thermal outcomes.

Based on the literature mentioned previously, it is found that water is the unique liquid used in all the studied DPSCs due to its availability and negligible cost. The relatively low heat capacity of water makes it incapable of retaining heat, especially during times of low sunlight. Moreover, water becomes unusable in extreme hot and cold climate conditions since it freezes at 0 °C and boils at 100 °C under atmospheric pressure. The knowledge gap addressed in this study revolves around the limited investigation into the performance of DPSCs using a variety of advanced HTFs beyond conventional water. The constraints associated with water motivated us to explore alternative liquids as no further investigations have been conducted for collectors using these alternatives. Furthermore, the author believes there is a scarcity of Computational Fluid Dynamics (CFD) studies on DPSCs. This study fills these gaps by numerically investigating the thermal behavior of a DPSC using ANSYS Fluent with three different working fluids: water, Therminol VP-1, and Dowtherm A. The present work aims to find the best alternative liquid to water that can be applied in DPSC. Therefore, the present work tested two different oil liquids alongside water as working fluids in DPSC, which is, thus, the first novelty of the work. Water, Therminol VP-1, and Dowtherm A have been examined numerically, adding another layer of innovation to the research. This study examines the simulation outcomes of a DPSC that incorporates seven circular liquid pipes and seven V-corrugated air ducts, employing water, Therminol VP-1, and Dowtherm A as HTFs. The present work investigates how different working liquids from the DPSC affect the outlet temperatures. Moreover, it examines the influence of various values of air flow rates on the exit temperatures, heat gains, and thermal efficacy of the DPSC, which are not extensively documented in existing literature. The current CFD simulation results gathered in this study are validated by comparing them with the experiments conducted by Assari et al. [23].

2. GEOMETRY OF THE DPSC AND CALCULATION METHOD

The geometry of the DPSC used in the current simulation study is the same as that designed by Assari et al. [23] (see Fig. 1). The collector consists of a single glass cover, an absorbent plate, seven lower-bonded parallel liquid tubes attached to the absorber plate, seven upper-bonded V-corrugated air channels attached to the top of the absorber and connected to the back insulation from the bottom.

Table 1 presents all the design variables related to the current simulated DPSC.

The total performance of the DPSC is evaluated by calculating the net heat obtained from its water and air parts. In general, the useful gain of the heat ($Q_{u,f}$) can be calculated as [24]:

$$Q_{u,f} = \dot{m}_f c_{p,f} \left(T_{o,f} - T_{i,f} \right), \tag{1}$$

where, $\dot{m}_f$, $c_{p,f}$, $T_{o,f}$, and $T_{i,f}$ are the mass flow rate, specific heat, exit, and input fluid temperatures. The subscript f stands for fluid, which is the water and air; therefore, the useful heat gained from the water part of the DPSC is:

$$Q_{u,w} = \dot{m}_w c_{p,w} \left(T_{o,w} - T_{i,w} \right) \tag{2}$$

and from the air side:

$$Q_{u,a} = \dot{m}_a c_{p,a} \left(T_{o,a} - T_{i,a} \right). \tag{3}$$

Thus, the total gain of heat for the DPSC is the algebraic sum of water and air heat gain [10]:

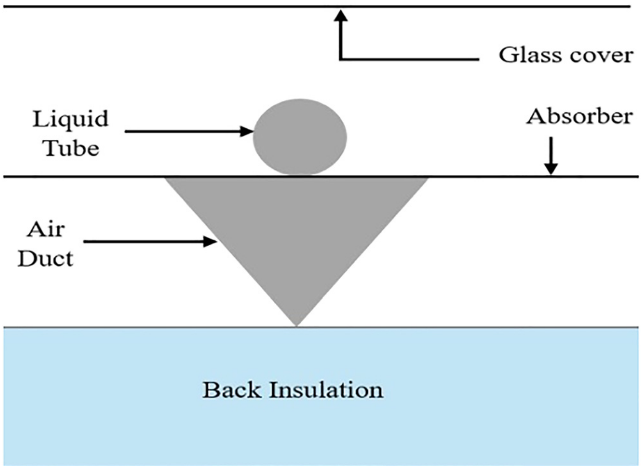

Fig. 1. Schematic of the studied DPSC system

Table 1. Geometric and material specifications of the studied DPSC [23]

Absorbent area	0.95 m × 1.9 4 m
Absorber	Aluminum sheet, 1 mm thickness
Pipe	Zinc material, 7 mm diameter
Airduct	Galvanized steel, Triangular with 6 cm height

$$Q_{u,D} = Q_{u,w} + Q_{u,a}. \tag{4}$$

The instantaneous thermal efficiency of the DPSC is:

$$\eta_D = \frac{Q_{u,D}}{A_c I_T} \cdot 100, \tag{5}$$

here, A_c denotes the area of the collector's absorbent plate and I_T stands for the total fallen radiation.

The present study considers Therminol VP-1 and Dowtherm A working fluids. Therminol VP-1 is an artificial heat transfer liquid characterized by its extraordinary thermal stability and low viscosity to guarantee effective, trustworthy, and regular performance across an optimum operational temperature range from 12 °C to 400 °C. It offers excellent thermal stability among natural HTFs [21]. The thermal features of these HTFs vary depending on the temperature. The thermo-physical features of Therminol VP-1 can be obtained from the following correlations [25], which is specifically designed for the range of (285.15 K ≤ T ≤ 698.15 K):

$$c_p = \begin{cases} 2.125 \cdot 10^3 - 11.017T + 0.049862T^2 \\ -7.7663 \cdot 10^{-5} T^3 + 4.394 \cdot 10^{-8} T^4, \end{cases} \tag{6}$$

$$\rho = \begin{cases} 1.4386 \cdot 10^3 - 1.8711T \\ +2.737 \cdot 10^{-3} T^2 - 2.3793 \cdot 10^{-6} T^3, \end{cases} \tag{7}$$

$$\lambda = \begin{cases} 0.14644 + 2.0353 \cdot 10^{-5} T \\ -1.9367 \cdot 10^{-7} T^2 + 1.0614 \cdot 10^{-11} T^3, \end{cases} \tag{8}$$

$$\mu = \begin{cases} 3.661 \cdot 10^2 - 3.0154T \\ +8.3409 \cdot 10^{-3} T^2 - 7.723 \cdot 10^{-6} T^3, \end{cases} \tag{9}$$

where, c_p, ρ, λ, and μ referred to the specific heat (J kg^{-1}·K), density (kg m^{-3}), thermal conductivity (W m^{-1}·K), and viscosity (mPa·s), respectively.

The correlations used to calculate the thermo-physical properties of Dowtherm A in the range of temperatures (288.15 K ≤ T ≤ 678.15 K) are given as follows [25]:

$$c_p = 911.4 + 2.011T + 9.368 \cdot 10^{-4} T^2, \tag{10}$$

$$\rho = 1190 - 0.2243T - 7.866 \cdot 10^{-4} T^2, \tag{11}$$

$$\lambda = 0.1856 - 1.6 \cdot 10^{-4} T, \tag{12}$$

$$\mu = 10^{5.274} T^{-3.247} + 10^{27.75} T^{-12.3}. \tag{13}$$

This study employs meticulously developed MATLAB code to compute the thermo-physical characteristics related to Therminol VP-1 and Dowtherm A liquids based on the above correlations in the range of temperatures 20–65 °C. The average value for each property is then imported into ANSYS Fluent software. The properties of all the materials (solids and fluids) utilized in the simulation are given in Table 2.

3. NUMERICAL MODELING

The current modeling process focuses on the collector, which features identical air ducts and water tubes.

Table 2. Thermophysical properties of the material and working fluids utilized in the simulation

Fluid	c_p, (J kg^{-1}·K)	ρ, (kg m^{-3})	λ, (W m^{-1}·K),	μ, (Pa·s)
Therminol VP-1	1609.73	1046.000	0.1339	0.0027
Dowtherm A	1698.53	1024.200	0.1315	0.0016
Aluminum	871.00	2719.000	202.4000	
Zinc	389.00	7140.000	116.0000	
Water	4182.00	998.200	0.6000	$1.0030 \cdot 10^{-3}$
Galvanized Steel	470.00	7850.000	52.0000	
Air	1006.43	1.2250	0.0242	$1.7894 \cdot 10^{-5}$

The three-dimensional geometry of the DPSC is built using the ANSYS Design Modeler. Half of a single air duct and water tube is modeled to optimize the approach. By incorporating symmetrical planes into the design, calculations could be simplified. This technique included building a semi-circular construction with a symmetric wall, substantially minimizing the required mesh elements. Consequently, this ensures improved mesh quality and simultaneously reduces the analysis processing time. The developed 3D geometry of DPSC is shown in Fig. 2. The model contains a half-liquid tube and a half-air channel.

The conformal mesh is generated, as shown in Fig. 3. The mesh is developed, consisting of tetrahedron elements with a structured mesh (prism layers) and a growth rate of 1.01. The boundary conditions of the studied model are defined by creating named selections in the Fluent meshing. Among these named boundaries, symmetry boundaries are helpful for minimizing the size of the computational domain. They are used when the physical geometry and the anticipated flow or thermal pattern show mirror symmetry.

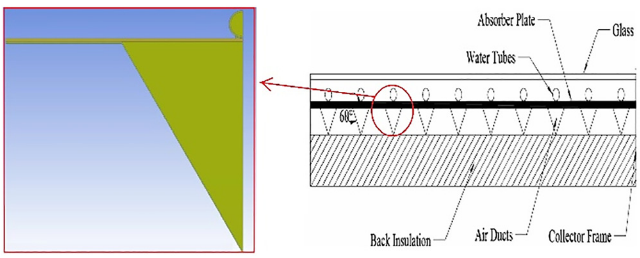

Fig. 2. The cross-sectional view of the DPSC and its corresponding ANSYS model

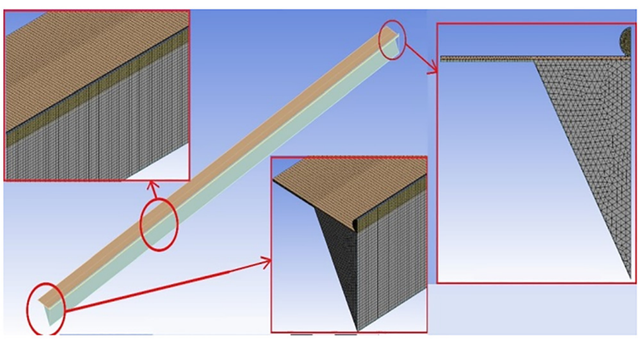

Fig. 3. Geometry and the mesh configuration for the studied DPSC

The mesh quality is rigorously tested using the conventional grid-independence test method. This test is a critical stage in CFD as it ensures that results depend on the physical model, not the mesh size [4]. The number of mesh elements increased from 595,182 to 1,334,844, and no considerable change in temperature after the increment of the number of elements after 1,308,692 (Fig. 4). The average mesh quality, skewness, and orthogonal quality are 0.78983, 0.12956, and 0.87791, respectively, which are considered suitable for computations, ensuring the reliability of our results [26].

The following assumptions are considered in the current investigation for the solution setup in ANSYS Fluent:

- The fluid flow is laminar, as the Reynolds number falling within the laminar regime;
- The fluid flow is steady, meaning its properties do not change with time;
- The properties of materials remain invariant with temperature changes;
- The fluids are assumed incompressible, meaning their density remains constant throughout the flow;
- Heat losses via the borders are discarded;
- No-slip condition is imposed on the system.

The energy equation is implemented with the laminar flow model, assuming a constant heat flux on the absorbent plate and a steady inlet fluid temperature. For numerical analysis, the pressure, momentum, and energy equations are discretized using a second-order upwind method. Gradient calculations are performed using the Green-Gauss node-based approach. Pressure-velocity coupling is achieved through a coupled scheme, while the remaining simulation

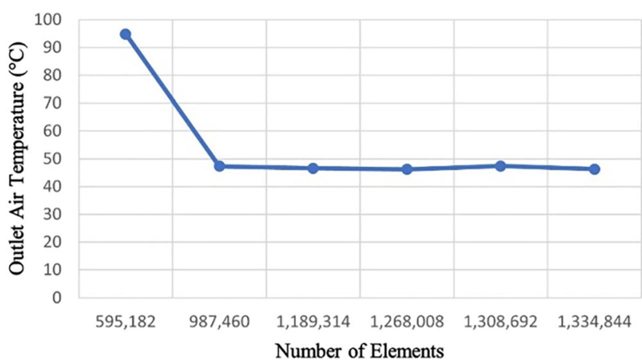

Fig. 4. Mesh independence test

settings are maintained at their default values. The residual criteria for the simulation are established with continuity and momentum set at 10^{-5}, and energy at 10^{-6}. Table 3 outlines the parameters employed as input boundary conditions in the present simulation. The liquid domain has fixed inlet conditions of 40 °C and a flow rate of 0.02 kg s^{-1}. In the air domain, the temperature at the inlet is set to 45 °C with variable mass flow rates to represent dynamic airflow conditions.

The numerical model forecasts the outlet air temperature and compares the numerical findings with experimental results obtained from [23]. The simulation is conducted at various air flow rates, keeping the other parameters constant. Figure 5 illustrates the disparity between experimental and numerical outcomes. The relative error is computed to demonstrate the convergence between simulated and experimental findings. The highest value of this error is 1.044%, while the minimum value is 0.085%.

4. RESULTS AND DISCUSSION

The DPSC with half a liquid tube and half of a V-corrugated air duct is simulated using ANSYS Fluent software. Three different liquids (water, Therminol VP-1, and Dowtherm A) have been utilized as heat transfer media for simulation. Identical operating parameters, as specified in Table 3, are employed for each case, with five air flow rate values that vary between 0.02 and 0.1 kg s^{-1} increased in increments of 0.02. Five simulation processes have been conducted for each case, which means 15 simulation processes have been conducted throughout this study. The analysis of how airflow rate affects the exit temperature of each examining liquid is shown in Fig. 6. The average temperature at the outlet is 45.32 °C when the inflow water temperature is 40 °C. In contrast, when utilizing Therminol VP-1 at the same inlet temperature, the average exit temperature increases to 51.82 °C. Similarly, Dowtherm's average outlet temperature is slightly lower at 51.53 °C.

It is observed that increasing the air flow rates has minimal effect on the exit temperatures of the studied liquids since the input air temperature is significantly greater than the liquid temperature, thereby, increasing airflow may not a substantial impact on reducing the exit liquid temperature. However, there is still a notable increase of 17.5%, 29.55%, and 28.83% in the outlet temperatures of the water, Therminol VP-1, and Dowtherm A, respectively, compared to the inlet liquid temperature of 40 °C. Notably, Therminol and Dowtherm demonstrate higher exit temperatures than water, with an average enhancement of 14.33% and 13.7%, respectively. The maximum outlet liquid temperature occurs at an airflow rate of 0.02 kg s^{-1}, while the inlet liquid temperature is 40 °C. These temperatures are 52.5 °C, 52 °C, and 45.6 °C for Therminol VP-1, Dowtherm A, and water, respectively.

The variation in airflow rate slightly impacts the outlet air temperature when the three liquids are utilized, as shown in Fig. 7. Increasing airflow decreases the residence time of the air in contact with the duct surface, thereby reducing the duration available for thermal exchange processes. This expedited airflow results in a lower outlet air temperature. The outlet air temperature when using Therminol is greater

Table 3. Input parameters and their corresponding values used in the numerical simulation [23]

Input parameter	Range
Solar irradiance	900 W m^{-2}
Inlet air temperature	45 °C
Inlet liquid temperature	40 °C
Air flow rate	0.02–0.1 kg s^{-1}
Liquid flow rate	0.02 kg s^{-1}

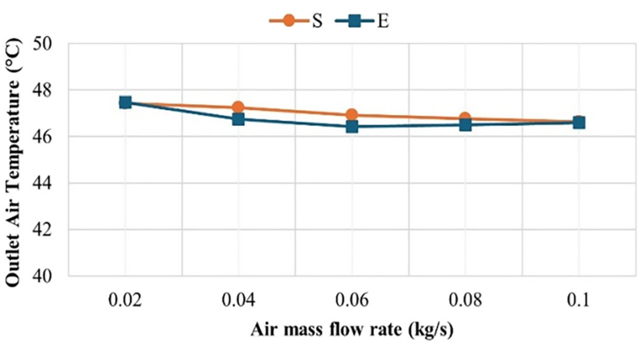

Fig. 5. Experimental validation of numerical results (S = Simulation, E = Experimental)

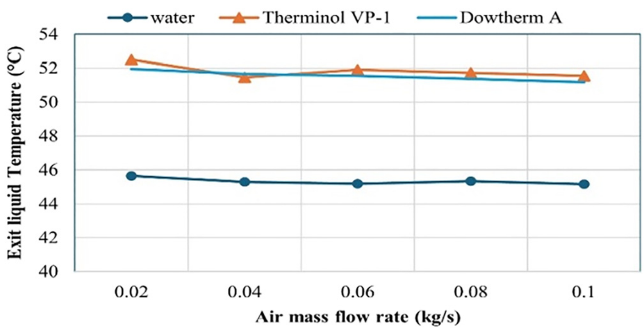

Fig. 6. The variation of exit liquid temperature with air flow rates

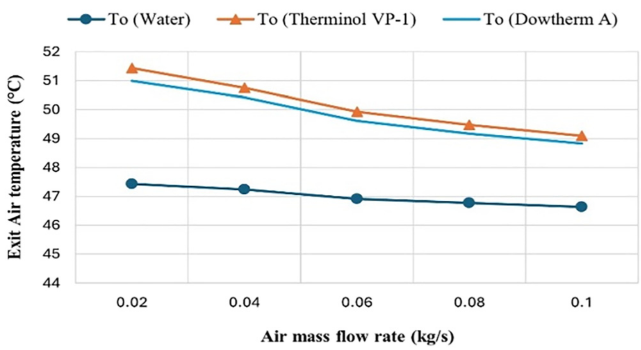

Fig. 7. The variance of exit air temperature with air flow rate

than that of water and Dowtherm. The average increase in exit air temperature is 6.67% for Therminol and 6% for Dowtherm relative to the case using water.

The maximum outlet air temperatures recorded are 51.4 °C, 51 °C, and 47.4 °C when using Therminol VP-1, Dowtherm A, and water, respectively. These temperatures occur at an airflow of 0.02 kg s^{-1}, with inlet air and liquid temperatures set at 45 °C and 40 °C, respectively. The high incident heat flux with the large surface area of the air duct and the low airflow allow the air temperature to rise significantly. The temperature contours for all domains (liquid tube, air duct, and absorber plate) of the DPSC are illustrated in Fig. 8 based on an air and water flow rate of 0.02 kg s^{-1}.

Therminol and Dowtherm exhibit similar temperature contours, as shown in Fig. 8a and b, ranging between 40 °C and 82 °C. Both liquids have nearly identical thermal conductivity and heat capacity, making distinguishing between their temperature contours difficult. The absorber plate reaches higher temperatures with Therminol and Dowtherm compared to water, and it continues to exhibit the highest temperature values for both the exit liquid and air. Conversely, the temperature contour of water varies between 40 °C and 62 °C. Additionally, water demonstrates more homogeneous behavior than Therminol and Dowtherm, likely attributed to its higher thermal conductivity and heat capacity, as depicted in Fig. 8c.

The beneficial thermal gain from the liquid and air sections of the DPSC is calculated using Eqs (2) and (3), respectively. As expected, the liquid heat gain remains relatively constant because the heat flux is constant, which means the heat transfer rate is stable. This stability arises from the consistent heat transfer coefficient and driving temperature difference. Moreover, the constant flow rate of the liquid ensures a uniform flow and, thereby, a stable convective heat transfer, which helps maintain a constant heat gain. Keeping the inlet liquid temperature constant ensures the heated pipe surface, which remains steady. In contrast, variations in airflow disrupt this stability, thereby increasing air heat gain with airflow rate. This can enhance the convection heat exchange between the air and the duct, as it is demonstrated in Fig. 9.

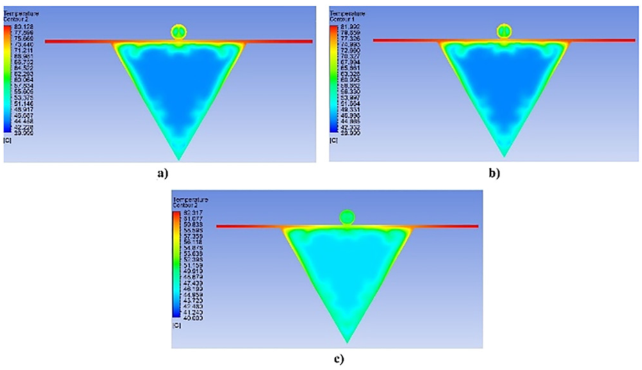

Fig. 8. Temperature contour of all domains of the DPSC when using three liquids: a) Dowtherm A, b) Therminol VP-1, and c) Water

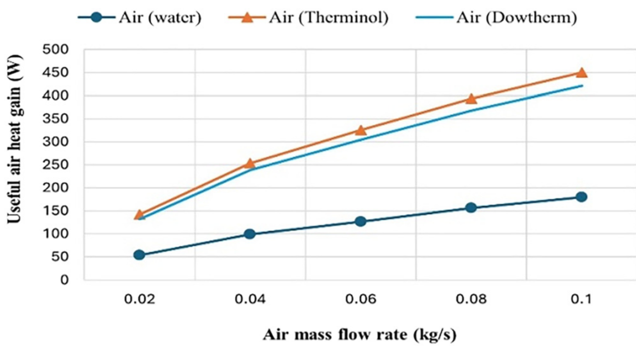

Fig. 9. The variance of useful air heat gain with air flow rates

As it is depicted in Fig. 9, Therminol VP-1 and Dowtherm provide advantages over water in terms of air heat delivery, as they exhibit lower heat capacities than water. This characteristic allows water to absorb the incident heat on the absorber more rapidly than the other two liquids, leaving less time for the air to heat up when using water. This difference is evident when comparing liquid heat delivery, illustrated in Fig. 10, where water shows the highest heat delivery values compared to Therminol and Dowtherm. Although water outperforms Therminol and Dowtherm A in heat gain from the liquid side of the DPSC, the total heat gain, representing the combined air and liquid heat gains for Therminol and Dowtherm, exceeds that of water.

The efficiencies of the liquid side, air side, and combined collector are presented in Figs 11–13, respectively. Efficiency is the proportion of beneficial heat obtained to the entire amount of irradiance hitting the absorber. It is evident from Figs 11 and 12 that the efficiencies of the air and liquid sides of the DPSC mirror the trends observed in useful gain since the incident radiation remains constant. For all values of the air flow rate, the liquid side efficacy when using water is greater than that of the other liquids.

The maximum air efficiency of Therminol VP-1, Dowtherm A, and water is 27.4%, 25.6%, and 10.9%, respectively, which corresponds to the highest air flow of 0.1 kg s^{-1}. These maximum air efficiency values are of significant

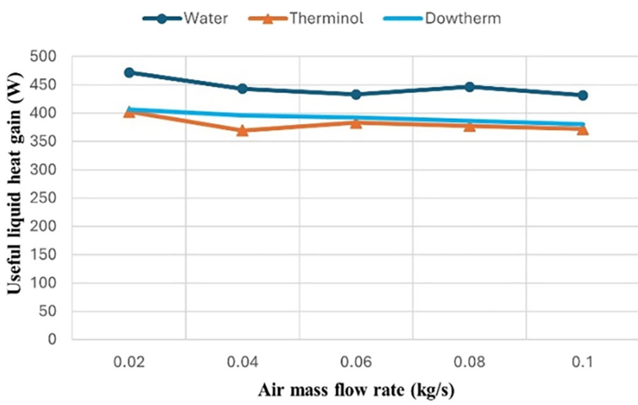

Fig. 10. The variance of liquid useful heat gain with air flow rates

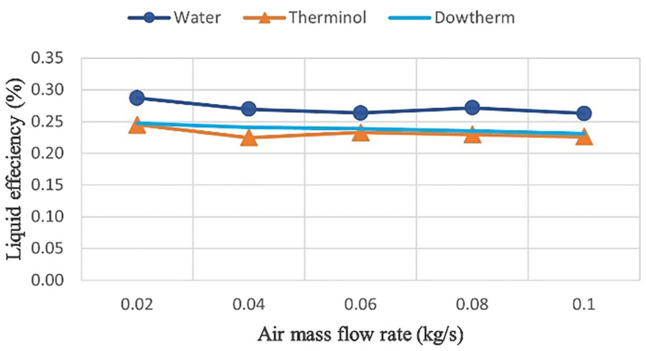

Fig. 11. The efficiency of the liquid side of the DPSC with an air flow rate

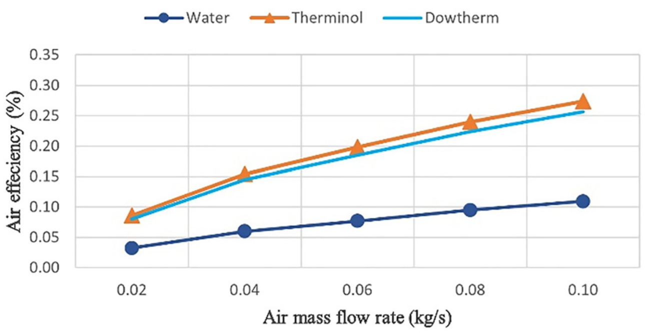

Fig. 12. The efficiency of the air side of the DPSC with an air flow rate

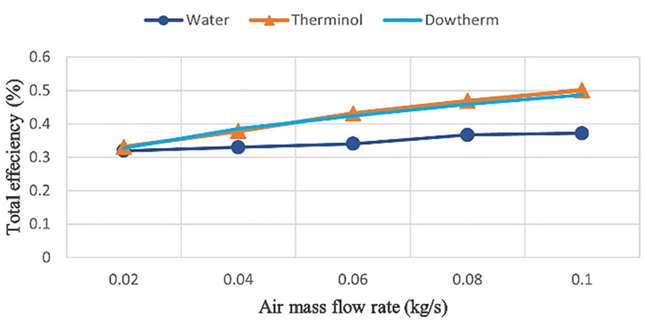

Fig. 13. Total efficiency of the DPSC with an air flow rate

importance as they directly impact the total thermal efficiency of the DPSC (see Fig. 13), which stands for the sum of the air and liquid sides' efficiencies as depicted in Eq. (4). The rise in air efficacy results from the higher air flow rate, which drops the temperature difference between the absorbent surface and the air. That minimizes the heat losses and maximizes the heat absorbed by the air.

The total efficiency of the DPSC is directly influenced by the increased airflow rate, particularly for both Therminol and Dowtherm liquids. Both liquids show a consistent increase in efficiency as the airflow rate rises, with the maximum efficiency recorded at 0.1 kg s^{-1}. This highlights the significant role of the airflow rate in the system's performance, as it influences the efficiency of both liquids.

5. CONCLUSION

In the present study, the DPSC is studied numerically using three different liquids in three simulation cases for five different air flow rates. Water, Therminol VP-1, and Dowtherm A are utilized as HTFs, each utilized in a single case and solved using ANSYS Fluent software, a computational fluid dynamics software widely used in thermal engineering research. Throughout this work, it is found that both Therminol VP-1 and Dowtherm A significantly enhance the exit air and liquid temperature, total heat gain, and overall thermal efficacy of the DPSC. Specifically, the median percentage enhancements of the exit air temperature are 6.67% for Therminol VP-1 and 6% for Dowtherm A, while the exit liquid temperatures show increases of 14.33% and 13.7%, respectively. Although increasing the air flow rate did not sensibly affect the exit liquid temperature, it resulted in decreased exit air temperatures. On the other side, the beneficial heat obtained from the liquid side of the DPSC when utilizing Therminol VP-1 and Dowtherm A is lower than that with water due to water's higher heat capacity, which enhances its capability of transferring the heat energy. However, the useful heat gain on the air side was greater with Therminol and Dowtherm, leading to higher overall total heat gains for these two HTFs compared to water. Notably, the thermal performance of the DPSC is superior when using Therminol VP-1 and Dowtherm A, achieving maximum enhancements in the thermal efficiency is 34.6% for Therminol and 31% for Dowtherm compared with water.

In summary, and based on the aforementioned findings, using Therminol and Dowtherm as HTF instead of water can efficiently ameliorate the gross thermal effectiveness of the DPSC. It is crucial to emphasize that although water offers the best temperature distribution, Therminol and Dowtherm have higher temperature values of the absorber plate, outlet air, and liquid. More investigations can be carried out by varying the other operating parameters, and their results can be discussed to confirm the robustness of these kinds of alternative liquids for use in solar thermal systems. Future recommended work includes conducting CFD simulations with varying liquid flow rates and a range of inlet fluid temperatures. Additionally, exploring a wider array of HTFs, including nanofluids and other innovative mixtures, may yield further insights into optimizing DPSC performance.

REFERENCES

[1] I. Omle, E. Kovács, and B. Bolló, "Applying recent efficient numerical methods for long-term simulations of heat transfer in walls to optimize thermal insulation," *Results Eng.*, vol. 20, 2023, Art no. 101476.

[2] I. Omle, A. H. Askar, E. Kovács, and B. Bolló, "Comparison of the performance of new and traditional numerical methods for

long-term simulations of heat transfer in walls with thermal bridges," *Energies*, vol. 16, no. 12, 2023, Art no. 4604.
[3] O. Al-Oran and F. Lezsovits, "Enhance thermal efficiency of parabolic trough collector using Tungsten oxide/Syltherm 800 nanofluid," *Pollack Period.*, vol. 15, no. 2, pp. 187–198, 2020.
[4] M. I. Afridi, A. O. Samarmad, M. Ali, F. L. Rashid, S. A. Kadhim, A. K. Jasim, D. R. Nayyef, E. S. Barrak, Y. Aryanfar, K. A. Hammoodi, and S. H. H. Karouei, "Numerical investigation on the performance of the solar air collector using jet impingement with W-shaped arrangement," *Case Stud. Therm. Eng.*, vol. 71, 2025, Art no. 106154.
[5] A. Ahmadi, M. A. Ehyaei, A. Doustgani, M. El Haj Assad, A. Hmida, D. H. Jamali, R. Kumar, Z. X. Li, and A. Razmjoo, "Recent residential applications of low-temperature solar collector," *J. Clean. Prod.*, vol. 279, 2021, Art no. 123549.
[6] M. M. Hasan and K. Hriczó, "A literature review of a dual-purpose solar collector," in *Selected Proceedings of the 4th Vechicle and Automotive Engineering*, Miskolc, Hungary, *Lecture Notes in Mechanical Engineering*, September 8–9, 2022, pp. 302–321.
[7] M. E. Zayed, J. Zhao, Y. Du, A. E. Kabeel, and S. M. Shalaby, "Factors affecting the thermal performance of the flat plate solar collector using nanofluids: A review," *Solar Energy*, vol. 182, pp. 382–396, 2019.
[8] E. Vengadesan and R. Senthil, "A review on recent developments in thermal performance enhancement methods of flat plate solar air collector," *Renew. Sustain. Energy Rev.*, vol. 134, 2020, Art no. 110315.
[9] M. R. Assari, H. B. Tabrizi, I. Jafari, and E. Najafpour, "An energy and exergy analysis of water and air with different passage in a solar collector," *Energy Sourc. A: Recovery, Utilization Environ. Effects*, vol. 36, no. 7, pp. 747–754, 2014.
[10] M. R. Assari, H. B. Tabrizi, H. Kavoosi, and M. Moravej, "Design and performance of dual-purpose solar collector," in *The Third International Exergy, Energy and Environment Symposium*, Evora, Portugal, July 1–5, 2007, pp. 1–6.
[11] *2009 ASHRAE Handbook: Fundamentals*. American Society of Heating, Refrigerating and Air-Conditioning Engineers, Inc. USA, 2009.
[12] M. Alktranee and P. Bencs, "Factors affecting nanofluids behavior: A review," *Int. Rev. Appl. Sci. Eng.*, vol. 14, no. 2, pp. 241–255, 2023.
[13] Y. Guo, Z. Mo, R. Zhang, D. Wang, and J. Fan, "Thermal-hydraulic performance of flat-plate solar collector plant using different heat-transfer fluids," *Energy Technology*, vol. 12, no. 8, 2024, Art no. 2400412.
[14] S. K. Verma and A. K. Tiwari, "Progress of nanofluid application in solar collectors: A review," *Energy Convers. Manag.*, vol. 100, pp. 324–346, 2015.
[15] M. S. Kamel and F. Lezsovits, "Experimental study on pool boiling heat transfer performance of magnesium oxide nanoparticles based water nanofluid," *Pollack Periodica*, vol. 15, no. 3, pp. 101–112, 2020.
[16] Y. Shang, K. A. Hammoodi, A. Alizadeh, K. Sharma, D. J. Jasim, H. Rajab, M. Ahmed, M. Kassim, H. Maleki, and S. Salahshour, "Artificial neural network hyperparameters optimization for predicting the thermal conductivity of MXene/graphene nanofluids," *J. Taiwan Inst. Chem. Eng.*, vol. 164, 2024, Art no. 105673.
[17] G. Sekrani and S. Poncet, "Ethylene- and propylene-glycol based nanofluids: A litterature review on their thermo-physical properties and thermal performances," *Appl. Sci.*, vol. 8, no. 11, 2018, Art no. 2311.
[18] F. M. Arslan and H. Günerhan, "Investigation of energetic and exergetic performances of parabolic trough collector with using different heat transfer fluids," *E3S Web of Conferences*, vol. 111, 2019, Art no. 01054.
[19] D. Balamurali and M. Natarajan, "Numerical-experimental analysis of solar liquid flat-plate collector with different HTF and internal grooves profiles in the absorber duct," *Appl. Solar Energy*, vol. 59, pp. 244–252, 2023.
[20] P. N. Prasad and S. Kalla, "Numerical investigation of solar flat plate collector using different working fluids," *Int. J. Ambient Energy*, vol. 44, no. 1, pp. 483–493, 2023.
[21] J. Alsarraf, A. A. Alnaqi, and A. A. A. A. Al-Rashed, "Simulation of two-phase hybrid nanofluid flow in a flat plate solar collector equipped with spiral absorber tube under the influence of magnetic field: Hydraulic-thermal, energy, and exergy analysis," *J. Magn. Magn. Mater.*, vol. 585, 2023, Art no. 171120.
[22] G. Kalaiarasi, R. Velraj, M. N. Vanjeswaran, and N. G. Pandian, "Experimental analysis and comparison of flat plate solar air heater with and without integrated sensible heat storage," *Renew. Energy*, vol. 150, pp. 255–265, 2020.
[23] M. R. Assari, H. B. Tabrizi, and I. Jafari, "Experimental and theoretical investigation of dual purpose solar collector," *Solar Energy*, vol. 85, no. 3, pp. 601–608, 2011.
[24] D. G. Gunjo, P. Mahanta, and P. S. Robi, "CFD and experimental investigation of flat plate solar water heating system under steady state condition," *Renew. Energy*, vol. 106, pp. 24–36, 2017.
[25] A. Mwesigye and İ. H. Yılmaz, "Thermal and thermodynamic benchmarking of liquid heat transfer fluids in a high concentration ratio parabolic trough solar collector system," *J. Mol. Liq*, vol. 319, 2020, Art no. 114151.
[26] I. Omle, A. H. Askar, and E. Kovács, "Optimizing the design of container house walls using argon and recycled plastic materials," *Buildings*, vol. 14, no. 12, 2024, Art no. 3944.